DEVELOPMENTAL DYNAMICS 243:712–729, 2014
DOI: 10.1002/DVDY.24103

Induction of the Ganglion Cell Differentiation Program in Human Retinal Progenitors Before Cell Cycle Exit

Marek Pacal, and Rod Bremner*

Lunenfeld Tanenbaum Research Institute, Mount Sinai Hospital, Toronto Department of Ophthalmology and Vision Sciences, Department of Laboratory Medicine and Pathobiology, University of Toronto, Toronto, Canada

Background: Despite the disease relevance, understanding of human retinal development lags behind that of other species. We compared the kinetics of gene silencing or induction during ganglion cell development in human and murine retina. **Results:** Induction of POU4F2 (BRN3B) marks ganglion cell commitment, and we detected this factor in S-phase progenitors that had already silenced Cyclin D1 and VSX2 (CHX10). This feature was conserved in human and mouse retina, and the fraction of Pou4f2^{+} murine progenitors labeled with a 30 min pulse of BrdU matched the fraction of ganglion cells predicted to be born in a half-hour period. Additional analysis of 18 markers revealed many with conserved kinetics, such as the POU4F2 pattern above, as well as the surprising maintenance of "cell cycle" proteins KI67, PCNA, and MCM6 well after terminal mitosis. However, four proteins (TUBB3, MTAP1B, UCHL1, and RBFOX3) showed considerably delayed induction in human relative to mouse retina, and two proteins (ISL1, CALB2) showed opposite kinetics, appearing on either side of terminal mitosis depending on the species. **Conclusion:** With some notable exceptions, human and murine ganglion cell differentiation show similar kinetics, and the data add weight to prior studies supporting the existence of biased ganglion cell progenitors. *Developmental Dynamics 243:712–729, 2014.* © 2013 Wiley Periodicals, Inc.

Key words: ganglion cell; retinal development; neuronal cell birth; gene induction; Ki67; Pou4f2

Submitted 28 October 2013; First Decision 29 November 2013; Accepted 2 December 2013; Published online 12 December 2013

Introduction

The timing and mechanism of the onset of neuronal differentiation are not completely understood. The retina is an ideal system to study these events as it is not essential for viability, and many genes have been identified that govern its development. In the mammalian retina, the various neuronal subtypes are born in a fixed and overlapping pattern, starting with the ganglion neurons (Bassett and Wallace, 2012). In the mouse, ganglion cells are generated approximately between embryonic day (E) 10.5 and postnatal day (P) 0, although the majority are born between E12 and E16 (Sidman, 1961; Young, 1985; Farah, 2004; Farah and Easter, 2005). Human retinal development is poorly understood compared with the rodent tissue, but retinogenesis begins approximately at the fifth fetal week (Fwk 5) (Barishak, 1992). Based on comparisons with other species it was predicted that ganglion cells are generated starting shortly after this date, peaking at ~ Fwk 8 and ending at ~ Fwk 12 (Workman et al., 2013). However, to our knowledge, no study has quantified the kinetics of ganglion cell birth in the human retina. As well as disease relevance, human retinal explants are also an appealing model to dissect kinetics because the slower developmental rate simplifies identification of intermediate steps.

A previous report indicated that the number of cells in the ganglion layer (GCL) stabilizes after Fwk 18 (Provis et al., 1985). Because approximately half of GCL cells are amacrine cells, ganglion cell genesis presumably ends some point before Fwk 18. Ganglion cells are generated from progenitors that undergo mitosis on the apical (outer) surface of the retina, and the newborn postmitotic neurons must migrate through the neuroblastic layer (NBL) to the basal (inner) surface and form the GCL. Here, therefore, we used the number migrating neurons in the NBL expressing the ganglion-specific POU-domain transcription factor POU4F2 (BRN3B) to approximate the extent of ganglion cell birth in the human retina.

Lineage analyses with retroviruses indicate that a single early embryonic retinal progenitor can generate a large clone of descendants containing multiple cell types, arguing that these cells are multipotent (Livesey and Cepko, 2001). However, late progenitors cannot generate early cell types when placed in an early environment, arguing that fate is intrinsically programmed. Indeed, well separated single progenitors plated in vitro generate all the usual retinal cell types, and in the same proportions as in vivo, again arguing that an intrinsic program drives development (Cayouette et al., 2003, 2006). An important

Grant sponsor: Canadian Institutes for Health Research; Grant number: 74570; Grant sponsor: Foundation Fighting Blindness Canada; Grant number: 531524.
*Correspondence to: Rod Bremner, Mount Sinai Hospital, Lunenfeld Tanenbaum Research Institute, 600 University Avenue, Room 840, Toronto, Ontario M5G 1X5. E-mail: bremner@lunenfeld.ca

Article is online at: http://onlinelibrary.wiley.com/doi/10.1002/dvdy.24103/abstract

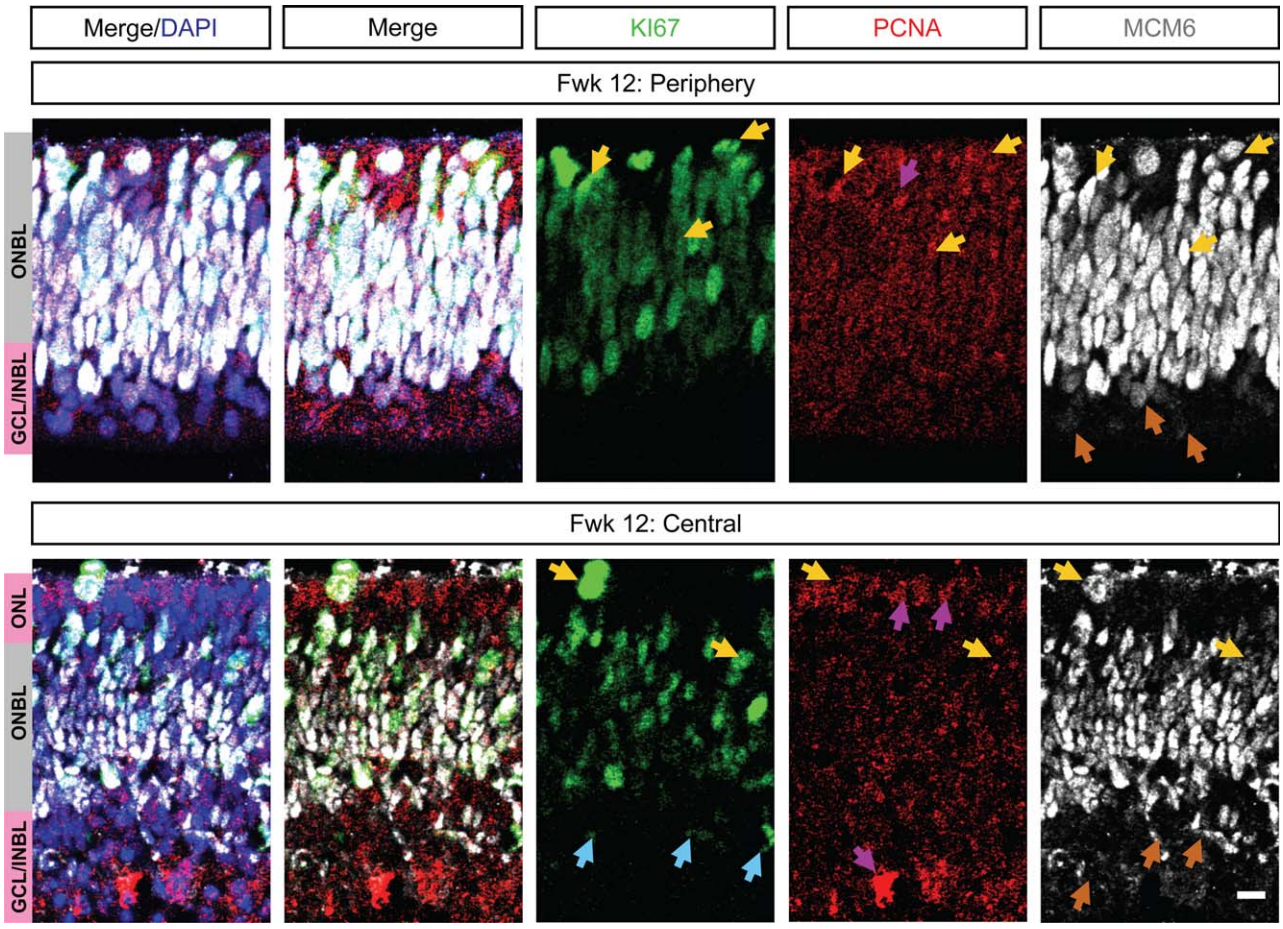

Fig. 1. The expression patterns of PCNA, MCM6, and KI67 in the human retina. At Fwk 12, KI67 (green), PCNA (red), and MCM6 (white) are mainly detectable and colocalize (yellow arrows) in the NBL, but they are not 100% confined to this region. KI67 is also detectable in the central INBL (blue arrows, lower panels). Strong PCNA staining is also detectable in the peripheral ONBL and central forming ONL and GCL (purple arrows). Many MCM6^{+} cells are located in the periphery and central INBL/GCL (orange arrows). Nuclei are also stained with DAPI (blue). ONL/INBL/ONBL/GCL: outer nuclear layer/inner neuroblastic layer/outer neuroblastic layer/ganglion cell layer. Scale bar = 10 μm.

outstanding issue in this intrinsic program is when exactly a progenitor loses pluripotency and becomes restricted such that it only produces one cell type or a specific lineage. Prior work has shown that even postmitotic retinal cells can be manipulated to change fate (Ezzeddine et al., 1997; Mizeracka et al., 2013), arguing that commitment is a very late event. However, there is also evidence from both zebrafish and mouse that some progenitors may be heavily biased to one or two specific fates before cell cycle exit (Poggi et al., 2005; Hafler et al., 2012).

Ganglion cells are an appealing model to study this problem because the onset of expression of the transcription factor Pou4f2 marks commitment to this lineage; thus, Pou4f2 is indispensable for ganglion cell specification, its overexpression promotes ganglion cell development, and is expressed specifically in ganglion cells (Xiang et al., 1993, 1995; Xiang, 1998; Liu et al., 2000; Qiu et al., 2008; Badea et al., 2009; Feng et al., 2011). Original studies on murine Pou4f2 suggested that its expression was limited to postmitotic cells that do not label with BrdU (Xiang, 1998; Pan et al., 2005), suggesting commitment to the ganglion cell lineage after cell birth. However, the proportion of all Pou4f2 cells that are born in the typically short (e.g., 30 min) period used for BrdU labeling is expected to be very small (see the Results section for details), and could be overlooked. Indeed, a recent study reported the detection of Pou4f2^{+} progenitors in the murine retina (Prasov and Glaser, 2012). Here, we show that, at least at early developmental times, POU4F2 is induced in human and murine S-phase progenitors after Cyclin D1 (CCND1) and VSX2 (CHX10) extinction, but before cell cycle exit. Analysis of an extensive panel of markers reveals many similarities in the kinetics of ganglion cell genesis in human vs. murine retina, including the maintenance of cell cycle proteins in migrating, postmitotic cells, and the gradual shift of the ganglion cell differentiation program to later times as development proceeds. However, we also define some noticeable differences, such as the induction of ISL1 (ISLET1) before or after mitosis in murine or human tissue, respectively, and the reverse species-specific pattern for CALB2 (Calretinin). Our results provide a useful framework for studying the timing of commitment to ganglion cell genesis in the human and mouse retina.

Results

KI67, Unlike PCNA and MCM6, is Mostly Confined to the NBL of the Fetal Human Retina

In the mouse retina, Pcna and Mcm6 are detected in the GCL as well as the NBL (Pacal and Bremner, 2012). As in murine retina, human

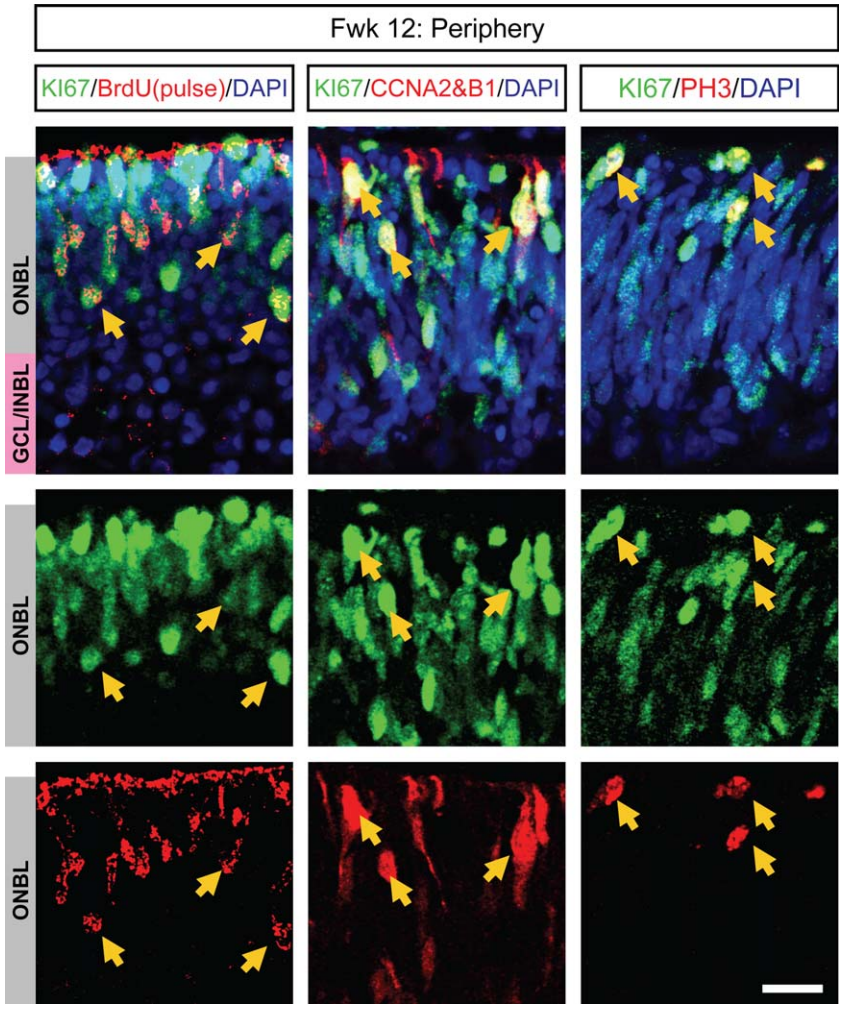

Fig. 2. KI67 is expressed in all phases of the cell cycle in human retinal progenitors. KI67 (green) colocalizes (yellow arrows highlight examples) with a short 30-min pulse of BrdU (red, S-phase) or cells positive for CCNA2 and B1 (A2 and B1 antibodies were combined; red, G2/M phase), or PH3 (red, M-phase). Nuclei are also stained with DAPI (blue). INBL/ONBL/GCL: inner neuroblastic layer/outer neuroblastic layer/ganglion cell layer. Scale bar = 10 μm.

PCNA and MCM6 were also detected beyond the ONBL in the forming GCL or the inner NBL (INBL) (Fig. 1). While the nuclear PCNA and MCM2 staining pattern are similar in murine retina (Pacal and Bremner, 2012), PCNA exhibited a more granular pattern than MCM2 in human Fwk 12 retina (Fig. 1). Also, compared with the mouse, where $Pcna^{+}$ cells are relatively sparse in the GCL, we found many strongly $PCNA^{+}$ cells in the human GCL, and also in the outermost part of the ONBL and the forming outer nuclear layer (ONL) (Fig. 1). Despite these subtle differences, these data suggest that MCM6 and PCNA are retained by some G0 differentiated neurons in both human and murine retina.

In the human retina, as in the murine tissue, KI67 was confined mainly to the outer neuroblastic layer (ONBL), although some inner NBL (INBL) cells were also positive (Fig. 1). However, unlike PCNA and MCM6, Ki67 was absent from the GCL (Fig. 1). This pattern could indicate that this protein is only present in progenitors, or that it is also expressed in postmitotic differentiating cells migrating through the ONBL (so-called G0* cells), as we saw before in the murine tissue (Pacal and Bremner, 2012). Assays to discriminate between these possibilities are outlined below.

KI67 is Detectable in All Phases of the Cell Cycle in the Fetal Human Retinal Progenitors

We first examined whether KI67 labels progenitors in all phases of the cells cycle. To label progenitors in different cell cycle phases we used a short pulse of BrdU (S-phase), or stained for Cyclins A2 and B1 (CCNA2&B1; G2/M-phase), or Ser10-phosphorylated histone 3 (PH3; M-phase), as described previously (Pacal and Bremner, 2012). These four markers displayed identical staining patterns in the mouse and human retina (Fig. 2), similar to a prior study (Lee et al., 2006). Furthermore, Ki67 colocalized with all of these four markers, indicating that this protein marks progenitors throughout the cell cycle (Table 1; Fig. 2).

A Fraction of $KI67^{+}$ Cells Lack the Pan Cell Cycle Markers CCND1 and VSX2 in the Fetal Human Retina

In the mouse retina, Ccnd1 and Vsx2 are detectable throughout the cell cycle in virtually all mouse retinal progenitors but a

TABLE 1. KI67 is Expressed in All Phases of the Cell Cycle in the Human Retina[a]

	BrdU pulse$^+$; KI67$^+$/BrdU pulse$^+$	CCNB1$^+$; KI67$^+$ /CCNB1$^+$	PH3$^+$;KI67$^+$ /PH3$^+$	VSX2$^+$;KI67$^+$ /VSX2$^+$	CCND1$^+$; KI67$^+$/CCND1$^+$
E12.5	1000/1000; 100 ± 0%	1000/1000; 100 ± 0%	1000/1000; 100 ± 0%	1000/1000; 100 ± 0%	1000/1000; 100 ± 0%
E14.5	1000/1000; 100 ± 0%	1000/1000; 100 ± 0%	1000/1000; 100 ± 0%	1000/1000; 100 ± 0%	1000/1000; 100 ± 0%
P0	1000/1000; 100 ± 0%	1000/1000; 100 ± 0%	1000/1000; 100 ± 0%	1000/1000; 100 ± 0%	1000/1000; 100 ± 0%

The percentage of marker$^+$/KI67$^+$ cells out of the total marker$^+$ population is shown. For example, all Ccnd1$^+$ cells were also KI67$^+$.

subset (6–7%) of mouse Ki67$^+$ retinal cells lack Ccnd1 and Vsx2, which are almost all differentiating G0* cells (Pacal and Bremner, 2012). We first examined the staining pattern of CCND1 and VSX2 in the human retina and then investigated whether all KI67$^+$ cells colabel with these markers. Later in retinal development VSX2 is expressed in bipolar and Muller cells (Burmeister et al., 1996; Rowan and Cepko, 2004). The predicted genesis of bipolar and Muller cells is ~ Fwk 10–25 and ~ Fwk 10–31, respectively (Workman et al., 2013). To ensure that we were labeling retinal progenitors with VSX2, and not bipolar or Muller cells, we examined early stages of retinal development before development of these cell types (Fwk 8) or when very few of these cell types would likely be born (Fwk 12). We found that CCND1 and VSX2 colabeled with, CCNA2&B1, PH3, or a short pulse of BrdU, indicating that they are present throughout the cell cycle in the human retinal progenitors (Fig. 3). Furthermore, in agreement with a previous study (Lee et al., 2006), we found that both CCND1 and VSX2 labeled a large number of cells throughout the entire NBL, indicating that they are present in the majority of progenitors. Similar to our findings in the mouse retina, a fraction of KI67$^+$ cells lacked VSX2 (e.g., Fwk 8 periphery 2.8 ± 0.1%) and a larger fraction was CCND1$^-$ (e.g., Fwk 8

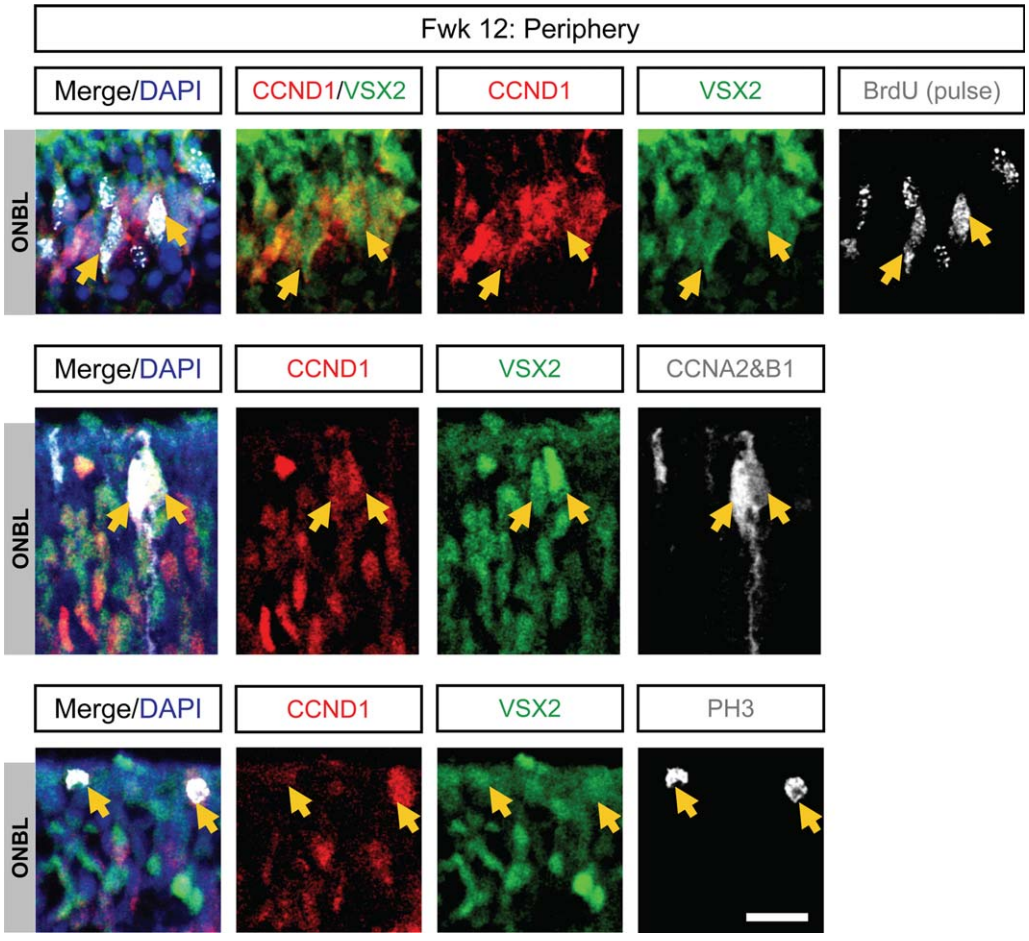

Fig. 3. The pan-cell cycle markers VSX2 and CCND1 label all phases of the cell cycle in human retinal progenitors. CCND1 and VSX2 colabel (arrows) with CCNA2&B1, PH3, or a short pulse of BrdU, indicating that they are present thought out the cell cycle in the human retinal progenitors. ONBL, outer neuroblastic layer. Nuclei are also stained with DAPI (blue). Scale bar = 10 μm.

TABLE 2. A Fraction of KI67$^+$ Cells in the Human Retina Lack VSX2 and/or CCND1[a]

	VSX2$^-$;KI67$^+$/KI67$^+$	CCND1$^-$;KI67$^+$/KI67$^+$
8 wk		
Central	18/900; 2.0 ± 0.3%	44/900; 4.8 ± 0.1%
Peripheral	26/900; 2.8 ± 0.1%	49/900; 5.4 ± 0.1%
12 wk		
Central	13/900; 1.4 ± 0.3%	41/900; 4.5 ± 0.1%
Peripheral	23/900; 2.5 ± 0.1%	46/900; 5.1 ± 0.1%

[a]The percentage of KI67$^+$;VSX2$^-$ or KI67$^+$;CCND1$^-$ cells out of the total KI67$^+$ population is shown. Thus, while all CCND1$^+$or VSX2$^+$cells were also KI67$^+$ (Table 1), not all KI67$^+$ cells were CCND1$^+$ or VSX2$^+$. Percentages represent the average of counts from at least three different retinas +/− SD.

periphery 5.4 ± 0.1%) (Table 2; Fig. 4). Furthermore, as in the mouse retina, some VSX2$^+$ cells were CCND1$^-$ (e.g., Fwk 8 periphery 3.1 ± 0.1%) while all CCND1$^+$ cells stained positive for VSX2 (Table 3; Fig. 4), suggesting that CCND1 is switched off before VSX2, possibly in progenitors about to exit the cell cycle. Moreover, the above data raise the possibility that KI67 is retained in some differentiating VSX2$^-$;CCND1$^-$ human neurons, as in the murine retina (Pacal and Bremner, 2012).

Quantification of Newborn Ganglion Cells in the Fetal Human Retina

The above data are consistent with the possibility that many or all the KI67 cells lacking CCND1 and VSX2 may be postmitotic differentiating neurons. To assess this issue, we decided to focus on differentiating ganglion cells. Prior work suggested that human ganglion cells are born between Fwk 5 and 18 (Workman et al., 2013). However, a detailed temporal quantification of human ganglion cell genesis has not been reported.

As in the mouse, POU4F2 (BRN3B) labels human ganglion cells (Lee et al., 2006). We used this marker to generate a histogram of migrating (i.e., newborn) ganglion cells in the peripheral and central NBL at eight developmental time points between Fwk 8 and 18 (Fig. 5A; Table 4). At Fwk 8, the peripheral NBL contained a small number of migrating POU4F2$^+$ cells where the GCL has yet to separate from the NBL. In contrast, the central Fwk 8 retina contained both migrating POU4F2$^+$ cells and an emerging GCL. These data are consistent with the prediction that human

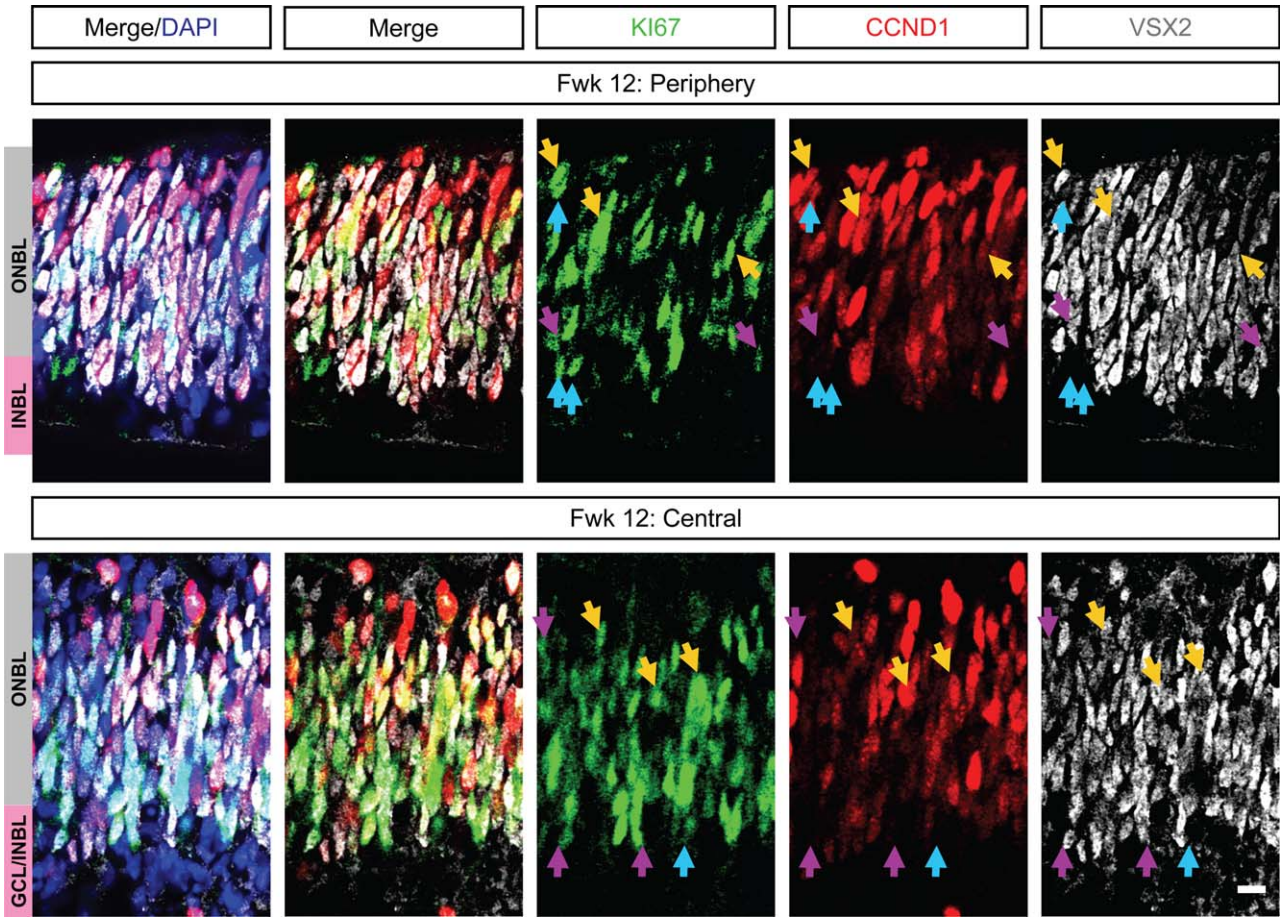

Fig. 4. A subset of KI67$^+$ cells lack the pan-cell cycle markers VSX2 and CCND1. The majority of KI67$^+$ cells (green) also colabeled (yellow arrows) with CCND1 (red) and VSX2 (white). However, a fraction of KI67$^+$ cells lacked CCND1 (purple arrows), VSX2, or both (blue arrows). Nuclei are also stained with DAPI (blue). ONBL/INBL/GCL: outer neuroblastic layer/inner neuroblastic layer/ganglion cell layer. Scale bar = 10 μm.

TABLE 3. A Small Population of VSX2$^+$ Cells in the Human Retina Lack CCND1[a]

	VSX2$^+$;CCND1$^-$/ VSX2$^+$	Ccnd1$^+$;VSX2$^-$/ CCND1$^+$
8 wk		
Central	36/900; 4.0 ± 0.3%	0/900; 0 ± 0%
Peripheral	28/900; 3.1 ± 0.1%	0/900; 0 ± 0%
12 wk		
Central	33/900; 3.6 ± 0.3%	0/900; 0 ± 0%
Peripheral	25/900; 2.7 ± 0.1%	0/900; 0 ± 0%

[a]The percentage of VSX2$^+$;CCND1$^-$ cells out of the total VSX2$^+$ population, and CCND1$^+$;VSX2$^-$ cells out of the total CCND1$^+$ cell population is shown. Percentages represent the average of counts from at least three different retinas +/− SD.

ganglion cell genesis begins around Fwk 5 in the central region (Barishak, 1992; Workman et al., 2013) (Fig. 5A,B). At Fwk 9, the GCL was also visible in the peripheral retina, indicating that progressively more ganglion cells are generated during this time. At Fwk 10, the number of migrating POU4F2$^+$ cells was highest and steadily decreased after this time point (Fig. 5A,B). After Fwk 16, very few migrating POU4F2$^+$ cells were observed. Thus, the majority of ganglion cells in the human retina are born between Fwk 9 and 12 and their genesis appears to end around Fwk 18, which fits with the previous report indicating that the GCL cell population stabilizes by ~Fwk 18 (Provis et al., 1985).

Induction of POU4F2 Before and ISL1 After Ganglion Cell Birth in Human Progenitors

Next, we assessed the timing of POU4F2 induction at Fwk 8 and 12 relative to cell cycle exit and to the appearance of ISL1, and POU4F1 (BRN3A), two other factors involved in ganglion cell differentiation (Xiang et al., 1995; Mu et al., 2008; Pan et al., 2008; Badea et al., 2009; Badea and Nathans, 2011). While POU4F1, which is restricted to the GCL, never colabeled with KI67, both POU4F2 and ISL1 did at both developmental stages examined (e.g., Fwk 8: POU4F2, 16.5 ± 1.5%; ISL1, 5.0 ± 1.0%) (Table 5; Fig. 6). More POU4F2$^+$ cells were KI67$^+$ than ISL1$^+$, suggesting that POU4F2 is induced before ISL1. In agreement, there were more migrating cells expressing POU4F2 than ISL1 (Fig. 6). Furthermore, a fraction of human POU4F2$^+$ cells colabeled with a short pulse of BrdU, or with CCNA2, CCNB1 or PH3 (Table 5; Fig. 6), but ISL1 never colabeled with cell cycle markers. Importantly, POU4F2$^+$ cells never colocalized with CCND1 or VSX2 (Table 5; Fig. 6). These data are consistent with a model in which human S-phase retinal progenitors that are about to exit the cell cycle switch off CCND1 then VSX2 and subsequently induce POU4F2, then once they exit the cell cycle and begin migrating/differentiating they up-regulate ISL1 (G0*), and as they reach their final destination they extinguish KI67 and induce POU4F1 (G0) (Fig. 7). Thus, in both murine and human embryonic retina, a fraction of KI67$^+$ cells are migrating, differentiating G0* neurons.

CALB2 is Induced Earlier in Human vs. Murine Retina While Other Human Neuronal Proteins Show Similar or Slower Kinetics

All the above human data mirror prior results showing that Ki67 expression is retained in postmitotic G0* mouse neurons until they complete their migration to the GCL (Pacal and Bremner, 2012). To further compare the kinetics of mouse vs. human ganglion cell genesis, we examined the early (Fwk 8) and mid (Fwk 12) stages of retinal development using eight neuronal markers expressed mainly in ganglion cells but also in other retinal neurons that were characterized previously with respect to their onset of detection in the mouse retina: TUBB3 (TUJ1), CALB2 (Calretinin), DCX (Doublecortin), ELAVL2/3/4 (HUC/D), MAP2, MTAP1B (MAP1B), UCHL1 (PGP9.5) and RBFOX3 (NEUN) (Pacal and Bremner, 2012) (for a summary see Fig. 7). PAX6, which labels both progenitors and neurons, served as a positive control for double labeling with KI67 (Fig. 8). In the murine retina, Ki67 colocalizes in G0* cells with five of the eight neuronal markers (Tubb3, Calb2, Dcx, Elval2/3/4, and Map2), while the other three (Mtap1b, Uchl1, and Rbfox3) are induced after Ki67 disappears (Pacal and Bremner, 2012) (Fig. 7). However, in human retina seven of the eight markers (TUBB3, DCX, ELVAL2/3/4, MAP2, MTAP1B, UCHL1, AND RBFOX3) were absent in KI67$^+$ cells and were mostly restricted to the GCL, suggesting induction in G0 cells (Fig. 8; Table 5); non-GCL KI67$^-$ cells expressing these markers are likely postmitotic horizontal cells or cones given their location (Fig. 8). Thus, four markers of neuronal development show delayed induction kinetics in human vs. mouse retinal ganglion cells. As in murine retina, human CALB2 colabeled with KI67 (e.g., Fwk 8 15.0 ± 3.5%; Fig. 8; Table 5). However, while all the Calb2$^+$;Ki67$^+$ cells in the embryonic murine retina are G0*differentiating neurons (Pacal and Bremner, 2012), we codetected human CALB2 with BrdU, CCNA2, CCNB1, or PH3, but not CCND1 or VSX2, suggesting induction in S-phase before cell cycle exit, but after CCND1 and VSX2 extinction (Fig. 9A). The kinetics of CALB2 appearance resemble that of POU4F2 and indeed, we found that ~60% of CALB2$^+$/BrdU$^+$ cells were also POU4F2$^+$ (Fig. 9B). CALB2$^+$;POU4F2$^-$ S-phase cells may be emerging human amacrine and/or horizontal cells because CALB2 is also expressed in these cell types (Nag and Wadhwa, 1999). In summary, the relative kinetics of induction of proteins associated with human ganglion cell differentiation is similar (MTAP1B, UCHL1, & RBFOX3), slower (TUBB3, DCX, ELVAL2/3/4, MAP2), or faster (CALB2) than in murine retina, and in the latter case occurs even before cell cycle exit (Fig. 7).

Both Pou4f2 and Isl1 are Expressed in Murine S-Phase Retinal Progenitors

The variable overlap of neuronal marker induction in human vs. murine tissue prompted us to examine the induction of the transcription factors Pou4f2, Isl1, and Pou4f1 in the mouse retina which, up to this point, we had only analyzed in human retina (Figs. 6, 7; Tables 4, 5). These factors are present in postmitotic cells (Xiang et al., 1995; Xiang, 1998; Pan et al., 2005, 2008), but recently Pou4f2 and Isl1 expression was also noted in a small subset of E11.5 and E13.5 retinal progenitors (Prasov and Glaser, 2012). As noted above, we found that human POU4F2 is induced in S-phase, after CCND1 and VSX2 extinction in progenitors, but that ISL1 is detected exclusively in postmitotic neurons (Figs. 6,

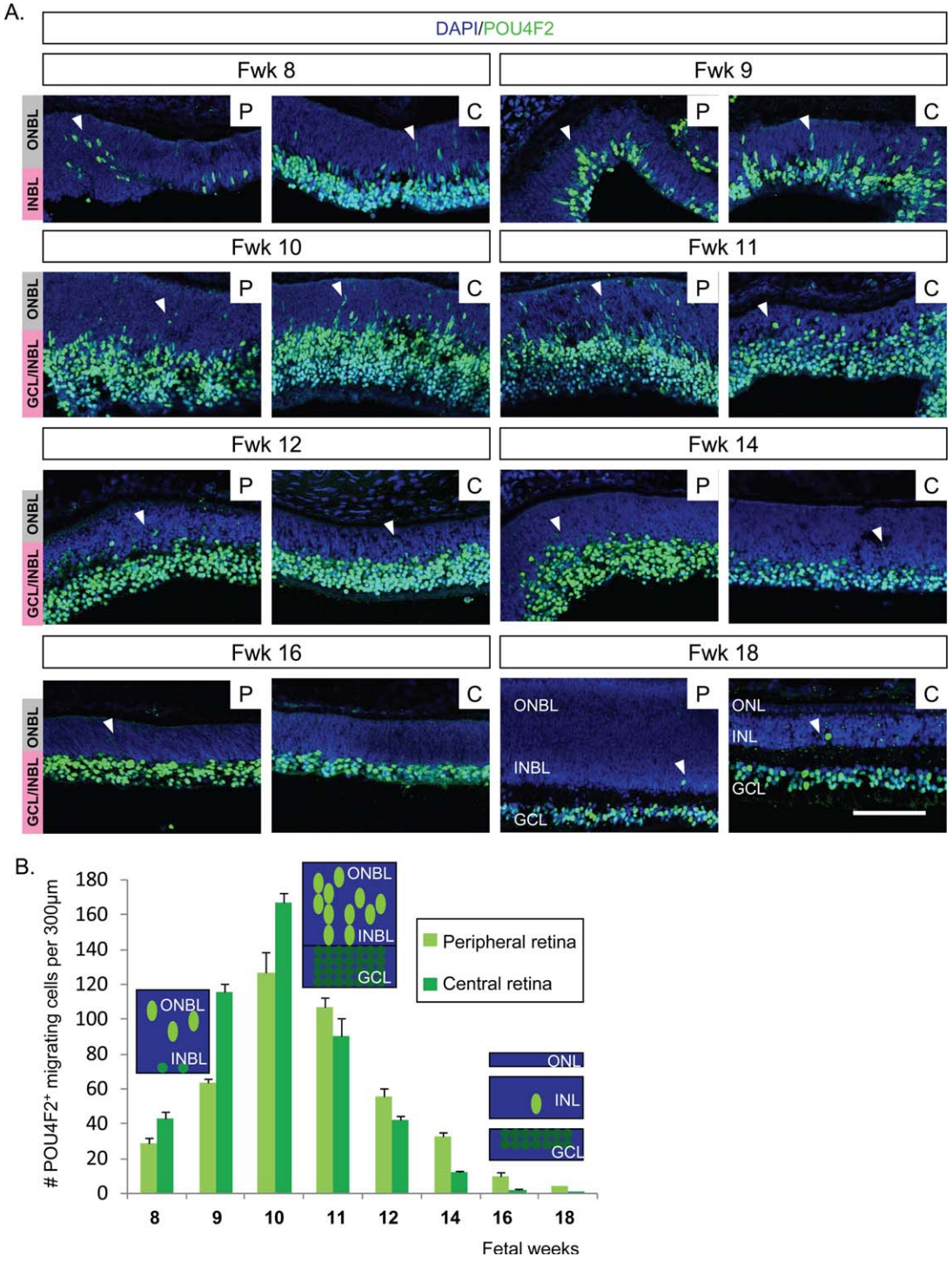

Fig. 5. Histogram of ganglion cell genesis in the human retina. **A:** We estimated the number of newborn ganglion neurons based on the number of migrating POU4F2$^+$ cells (white arrowheads). **B:** The values were obtained from three different sections, the error bars represent standard deviation. The cartoons within the histogram depict the typical retinal architecture and the number of POU4F2$^+$ cells observed at the early, mid and late stages of the human ganglion cell development. ONBL/INBL/GCL: outer neuroblastic layer/inner neuroblastic layer/ganglion cell layer. Scale bar = 100 μm.

7; Table 5). In the murine E12.5 retina, the NBL contained many migrating Pouf4f2$^+$ and Isl1$^+$ cells but much fewer Pou4f1$^+$ cells (Fig. 10). Accordingly, significant fractions of mouse Pouf4f2$^+$ and Isl1$^+$ cells colabeled with Ki67 (15.4 ± 2.5% and 12.4 ± 0.7%, respectively), while only a minute fraction of E12.5 Pou4f1$^+$ cells were Ki67$^+$ (0.1 ± 0.0%) which were close to the GCL (Fig. 10A; Table 6). At later times, all mouse Pou4f1$^+$ cells were in the GCL and lacked Ki67, confirming its status as a later marker of ganglion cell differentiation (Table 6). At E14.5, the fraction of Pouf4f2$^+$ or Isl1$^+$ cells that also labeled with Ki67$^+$

TABLE 4. Quantification of Migrating POU4F2$^+$ Cells[a]

	POU4F2$^+$cells per 300 μm		
Time point	Peripheral	Central	Average
Fwk 8	28.6 ± 3.2%	42.6 ± 4.1%	35.6 ± 8.3%
Fwk 9	63.0 ± 2.6%	115.0 ± 5.0%	89.0 ± 28.7%
Fwk 10	126.6 ± 11.5%	166.6 ± 5.7%	146.6 ± 23.3%
Fwk 11	106.6 ± 7.7%	90.0 ± 10.0%	98.3 ± 11.6%
Fwk 12	55.0 ± 5.0%	41.6 ± 2.8%	48.3 ± 8.1%
Fwk 14	32.6 ± 2.5%	12.0 ± 1.0%	22.3 ± 11.4%
Fwk 16	9.6 ± 2.0%	1.6 ± 0.5%	5.6 ± 4.5%
Fwk 18	3.6 ± 0.5%	1.0 ± 0.0%	2.3 ± 1.5%

[a]The average number of POU4F2$^+$cells in 3 different regions of peripheral and central retina, respectively, and the average of these two combined, at 8 different developmental stages. Percentages represent the average of counts from at least three different retinas +/− SD.

was reduced (2.2 ± 0.1% and 2.5 ± 0.5%, respectively). This shift is seen with multiple markers in both human and murine retina (Tables 5, 6; Fig. 7) (Pacal and Bremner, 2012) arguing that the kinetics of ganglion cell differentiation is delayed as the retina develops. At E16.5, Pou4f2$^+$ cells no longer colocalized with Ki67, and although we observed an increase in the proportion of Isl1$^+$;Ki67$^+$ cells at this time point (16.1 ± 2.5%), this likely reflects the large rise in amacrine cell births at E16.5 (Young, 1985), because Isl1 labels cholinergic amacrine cells (Galli-Resta et al., 1997; Elshatory et al., 2007).

Next, we asked whether the Ki67$^+$ population expressing these three transcription factors were progenitors or G0* neurons. As in human tissue, Pou4f1$^+$ cells never colocalized with BrdU, Ccna2/b1, PH3, Ccnd1, or Vsx2, suggesting that the few Pou4f1$^+$/Ki67$^+$ cells were G0* ganglion neurons (Fig. 10B; Table 6). In agreement, using a BrdU-chase and knowledge of the maximum G2/M length (E12.5: 90 min, E14.5: 110 min, E16.5: 130 min) (Pacal and Bremner, 2012), we found that Pou4f1 was first detectable ~8–10 hr after the last G2/M at E12.5 and E14.5, and ~10–22 hr at E16.5, a significant amount of time after cell birth (Fig. 10C; Table 6). Unlike Pou4f1, a small fraction of both murine Pou4f2$^+$ and Isl1$^+$ cell populations colabeled with BrdU (1.5 ± 0.0%), Ccna2/b1, and PH3 (0.2 ± 0.0% and 0.2 ± 0.1%, respectively) (Fig. 11A–D; Table 6). These data suggest that Pou4f2 follows similar induction kinetics in S-phase in both human and murine retina, but whereas human ISL1 is induced after cell cycle exit, murine Isl1 is induced at the same time as Pou4f2 (Fig. 7). Notably, the BrdU-labeled Pou4f2$^+$ and Isl1$^+$ cells were devoid of Ccnd1 and Vsx2 (Fig. 11A,B; Table 6), also mimicking the expression pattern of POU4F2 in the human retina (Fig. 6; Table 5). In agreement, we previously reported that, at E12.5 but not later, a fraction of murine PH3$^+$ G2/M progenitors colabels with the neuronal marker Tubb3, but is devoid of both Vsx2 and Ccnd1 (Pacal and Bremner, 2012), and here we found that these ventricular G2/M Tubb3$^+$ cells (either PH3$^+$ or labeled by a 1.5-hr BrdU pulse, which corresponds to the length of G2/M at E12.5; Pacal and Bremner, 2012) were also Pou4f2$^+$ and Isl1$^+$ (Fig. 11E,F).

In summary, while the kinetics of Pou4f1 or 2 induction is similar in human and murine retina, Isl1 is induced earlier in mice (Fig. 7A,D). The presence of multiple human (POU4F2, CALB2) or murine (Pou4f2, Isl1, Tubb3) neuronal markers in BrdU$^+$;Ccna2/B2$^+$;PH3$^+$ progenitors that lack VSX2 and CCND1 supports the notion that these may be biased progenitors fated to exit the cell cycle and become ganglion cells.

The above data show that around 1–2% murine Pou4f2$^+$ cells are progenitors as defined by labeling with a half-hour pulse of BrdU at E12.5 (Table 6). If these are fated to become ganglion cells, then the fraction of such cells born every half hour should also be 1–2%. Murine ganglion cell births begin at E10.5 (Young, 1985; Farah and Easter, 2005) thus assuming a linear birth rate, 1.04% of all those born in the next 2 days (i.e., up to E12.5) are born each half hour (100%/48 hr/2), which resembles the 1.5% of Pou4f2$^+$ or Isl1$^+$;BrdU$^+$ cells we detected (Table 6). The total number of ganglion cells generated by E11.8 or E12.8 is 3,589 or 9,793, respectively (Farah and Easter, 2005), suggesting a slight deviation from linear expansion (polynomial trend-line $y = 2.27x^2 + 95.06x$ - 6E-13; Fig. 11G). Focusing on the 0.5 hr just before E12.5 (i.e., the time of our BrdU labeling, 47.5–48 hr), substituting 47.5 for x gives 9,637 cells. Thus, the number of cells born between 47.5 and 48 hr is 156 (9,793–9,637), which represents 1.59% (100 x 156/9,793) of the total born by E12.5. This fraction is almost identical to the 1.5% of Pou4f2$^+$ (or Isl1$^+$) cells we observed in the S-phase at E12.5. These approximations are consistent with the notion that Pou4f2$^+$/Isl1$^+$ S-phase progenitors are fated to become ganglion cells.

Discussion

Human retinal development has not been well characterized, but is generally assumed to follow a pattern similar to that observed in other better studied mammals. Here, we characterized human ganglion cells, and found that their emergence peaks at Fwk 12 and is essentially over by Fwk 18. Detailed marker analysis here reveals several similarities and some notable differences between human and murine ganglion cell development, and exposes several distinct steps in the kinetics of protein extinction and induction during human ganglion cell production (Fig. 7). Moreover, as discussed below, our data lend support to the idea that ganglion cell generation, at least at earlier phases of retinogenesis, may be decided before cell cycle exit.

Molecular Kinetics of Human and Murine Ganglion Cell Development

In human and murine retina, we find that CCND1 disappears in progenitors before VSX2, and both events occur in S-phase, presumably as these cells are about to become postmitotic. In support of the latter model, both human Fwk 8 and murine E12.5 retina exhibit POU4F2$^+$ S-phase cells that are CCND1$^-$;VSX2$^-$, arguing that at these early developmental times POU4F2 is induced after VSX2 extinction and before cell cycle exit. Formally, we cannot exclude the notion that CCND1$^-$;VSX2$^-$;POU4F2$^+$ progenitors reactivate CCND1/VSX2, switch off POU4F2, and re-enter the cell cycle. Nevertheless, combining our E12.5 analyses with prior quantification of murine ganglion cell generation (Pacal and Bremner, 2012) revealed that ~1.5% of ganglion cells are born each half hour, which closely matches the fraction of POU4F2$^+$ progenitors we observed at this

TABLE 5. Colocalization of Neuronal and Cell Cycle Markers in the Human Retina [a]

	KI67	A short BrdU pulse	CCNB1	PH3	VSX2
Marker/age	Marker$^+$; KI67$^+$/Marker$^+$	Marker$^+$; BrdU$^+$ /Marker$^+$	Marker$^+$; CCNB1$^+$ /Marker$^+$	Marker$^+$; PH3$^+$ /Marker	Marker$^+$; VSX2$^+$ /Marker
PAX6					
8wk	211/450; 46.8 ± 1.6%	159/600; 26.5 ± 1.3%	27/600; 4.5 ± 0.5%	7/600; 1.1 ± 0.2%	231/600; 38.5±1.0%
12wk	217/500; 43.6 ± 2.8%	127/600; 21.1 ± 1.8%	25/600; 4.1 ± 0.7%	6/600; 1.0 ± 0.5%	238/600; 39.6±2.9%
POU4F2 (BRN3B)					
8wk	82/495; 16.5 ± 1.5%	4/1200; 0.3 ± 0.1%	4/1200; 0.3 ± 0.1%	4/1200; 0.3 ± 0.1%	0/1200; 0 ± 0%
12wk	8/580; 1.3 ± 0.3%	3/1200; 0.25 ± 0.0%	3/1200; 0.25 ± 0.0%	3/1200; 0.25 ± 0.0%	0/1200; 0 ± 0%
CALB2 (CALRETININ)					
8wk	84/540; 15.0 ± 3.5%	4/1200; 0.3 ± 0.1%	4/1200; 0.3 ± 0.1%	4/1200; 0.3 ± 0.1%	0/1200; 0 ± 0%
12wk	46/500; 10.7 ± 4.1%	4/1200; 0.3 ± 0.1%	4/1200; 0.3 ± 0.1%	4/1200; 0.3 ± 0.1%	0/1200; 0 ± 0%
ISL1 (ISLET1)					
8wk	30/500; 5.0 ± 1.0%	0/900; 0 ± 0%	0/900; 0 ± 0%	0/900; 0 ± 0%	0/900; 0 ± 0%
12wk	5/600; 0.8 ± 0.2%	0/900; 0 ± 0%	0/900; 0 ± 0%	0/900; 0 ± 0%	0/900; 0 ± 0%
MAP2					
8wk	0/600; 0 ± 0%				
12wk	0/600; 0 ± 0%				
DCX2 (DOUBLECORTIN)					
8wk	0/600; 0 ± 0%				
12wk	0/600; 0 ± 0%				
ELAVL2/3/4 (HUC/D)					
8wk	0/600; 0 ± 0%				
12wk	0/600; 0 ± 0%				
UCHL1 (PGP9.5)					
8wk	0/600; 0 ± 0%				
12wk	0/600; 0 ± 0%				
TUBB3 (TUJ1)					
8wk	0/600; 0 ± 0%				
12wk	0/600; 0 ± 0%				
RBFOX3 (NEUN)					
8wk	0/600; 0 ± 0%				
12wk	0/600; 0 ± 0%				
MAP1					
8wk	0/600; 0 ± 0%				
12wk	0/600; 0 ± 0%				

[a]The percentage of cells positive for 11 neuronal markers and the five cell cycle markers are shown. The markers and developmental stages examined are indicated in the first column; thus for PAX6 at Fwk 8, in the column labeled KI67, of 450 PAX6$^+$ cells 211 were also KI67$^+$. The pale orange highlighting indicates colocalization of neuronal and proliferation markers. Percentages represent the average of counts from at least three different retinas +/− SD.

stage. Together, the simplest interpretation is that CCND1$^-$;VSX2$^-$;POU4F2$^+$ progenitors generate postmitotic, differentiating ganglion cells. In further support of pre–M-phase activation of the ganglion cell program, we detected the ganglion/neuronal marker CALB2 with POU4F2 in cycling CCND1$^-$; VSX2$^-$ human progenitors.

Our data also indicate that the above events in human progenitors are followed in postmitotic migrating cells with induction of the ganglion cell determinant ISL1. In murine retina, Isl1 and Calb2 show the reverse order of appearance, with Isl1 present already in Ccnd1$^-$;Vsx2$^-$;Pou4f2$^+$ S-phase progenitors (this work), and Calb2 limited to the postmitotic migratory phase (Pacal and Bremner, 2012). These are intriguing differences in the species specific program, but both datasets support the notion that the differentiation program begins before cell cycle exit (see next section for further discussion).

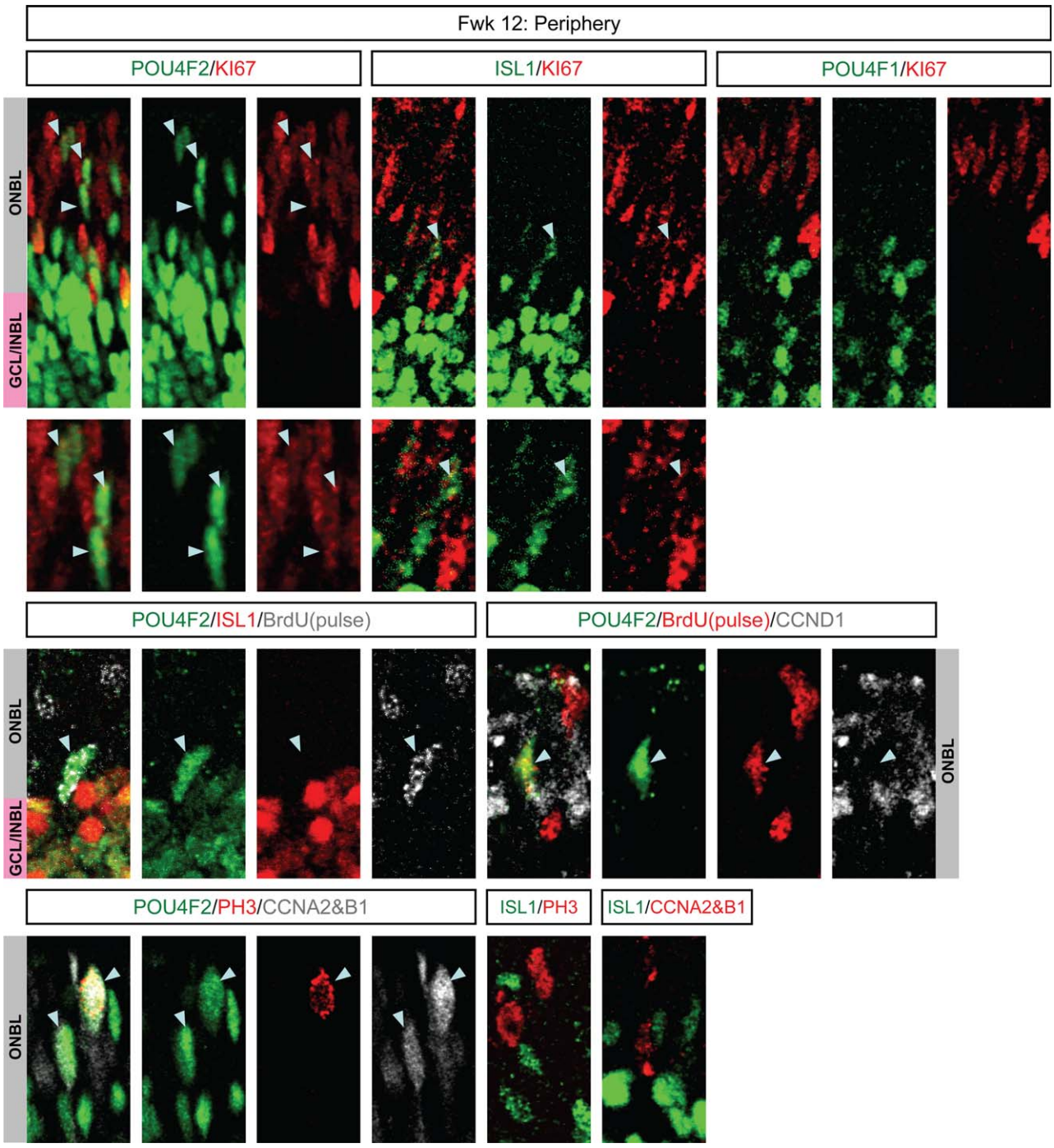

Fig. 6. Kinetics of POU4F2, ISL1, and POU4F1 induction in human fetal retina. Top panel: POU4F2 or ISL1 but not POU4F1 (green) colabeled Ki67 (red). Middle panel: POU4F2 colocalizes with BrdU (white, left; red, right) but not CCND1 (white, right). Bottom panel: POU4F2 (green) but not ISL1 (green) colocalizes with CCNA2/B1 (white left, red, right) or PH3 (red). INBL/ONBL/GCL: inner neuroblastic layer/outer neuroblastic layer/ganglion cell layer. Arrows indicate examples of cells colabeled with at least two markers. Scale bar = 10 μm.

At later ages (e.g., Fwk 12 or E14.5), there were fewer human and no murine POU4F2^{+} progenitors. These data are consistent with many other markers in this and prior works (Brzezinski et al., 2012; Pacal and Bremner, 2012) indicating that the kinetics of ganglion cell differentiation slows as retinal development proceeds, with the earliest events shifting from before to after cell cycle exit, and later events moving further in time from the final mitosis. A consistent feature of postmitotic ganglion cell differentiation in humans and mice is that KI67 only disappears once G0* cells arrive at their final destination in the GCL, and this conversion to G0 coincides with the induction of the ganglion cell-specific transcription factor POU4F1. These data, as well as the even longer retention of PCNA and MCM6, support the notion that differentiating cells retain some cell cycle features for a

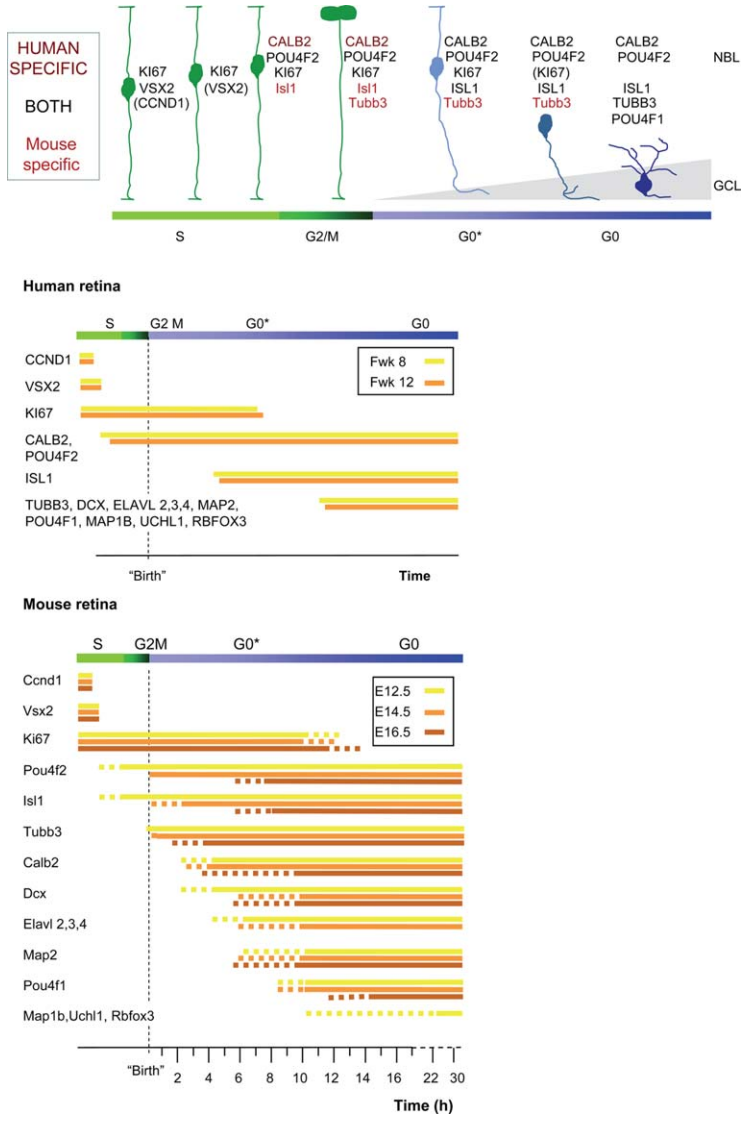

Fig. 7. Summary of marker induction in the human fetal and mouse embryonic retinas. The upper panel provides a schematic representation of a section through the early embryonic retina, and summarizes the kinetics of a subset of the markers studied, highlighting human: mouse differences in ganglion cell genesis. Progenitors are green while postmitotic differentiating cells are blue. Markers in parenthesis will disappear in the next step to the right. Proteins with different kinetics in human vs. mouse are indicated in red. NBL, neuroblastic layer; GCL, ganglion cell layer. The lower panels provide a comprehensive summary of the timing of protein induction/extinction in human and murine retina at multiple time points using data from this and prior (Pacal and Bremner, 2012) work. Line colors represent the kinetics at different times in development, as indicated in the legend. For the human data, each marker is shown relative to other markers and precise times were not obtained. For the murine data, marker induction relative to end of M-phase was assessed using BrdU chase times (this work and Pacal and Bremner, 2012). The dotted portion of each colored line indicates the two time points in the BrdU chase between which the marker appears or, in the case of Ki67, disappears.

lengthy period after final mitosis (Pacal and Bremner, 2012). This property may facilitate abnormal division of differentiating RB deficient neurons (Chen et al., 2004, 2007; MacPherson et al., 2004), a critical prelude to transformation and retinoblastoma (Sangwan et al., 2012). Moreover, the shift to commitment beyond M-phase as specific populations emerge may also enhance plasticity of differentiating cells, and this could also enhance sensitivity to neoplastic transformation.

The loss of KI67 and induction of POU4F1 in the human GCL is conserved in mice, as is the late induction of the ganglion/neuronal markers MTAP1B, UCHL1, and RBFOX3 (Fig. 7) (Pacal and Bremner, 2012). Moreover, retention of the cell cycle proteins PCNA and MCM6 in both migrating and mature ganglion cells is also conserved. However, whereas in humans four other neuronal proteins (TUBB3, MTAP1B, UCHL1, and RBFOX3) are also induced only in the GCL, these proteins appear earlier in the mouse. Thus, murine Tubb3 is detectable as early as G2/M at E12.5, and then in migrating postmitotic neurons at later stages, and murine Dcx, Elavl2/3/4 and Map2 are also already detectable in migrating $Ki67^{+}$ G0* mouse neurons (Fig. 7) (Pacal and Bremner, 2012).

In summary, our assessment of ganglion cell genesis indicates similar expression patterns for 12/18 proteins, including extinction of CCND1, VSX1, KI67, PCNA, and MCM6, and induction of POU4F2, POU4F1, MTAP1B, UCHL1, and RBFOX3. However, CALB2 and ISL1 show opposite kinetics in human vs. murine

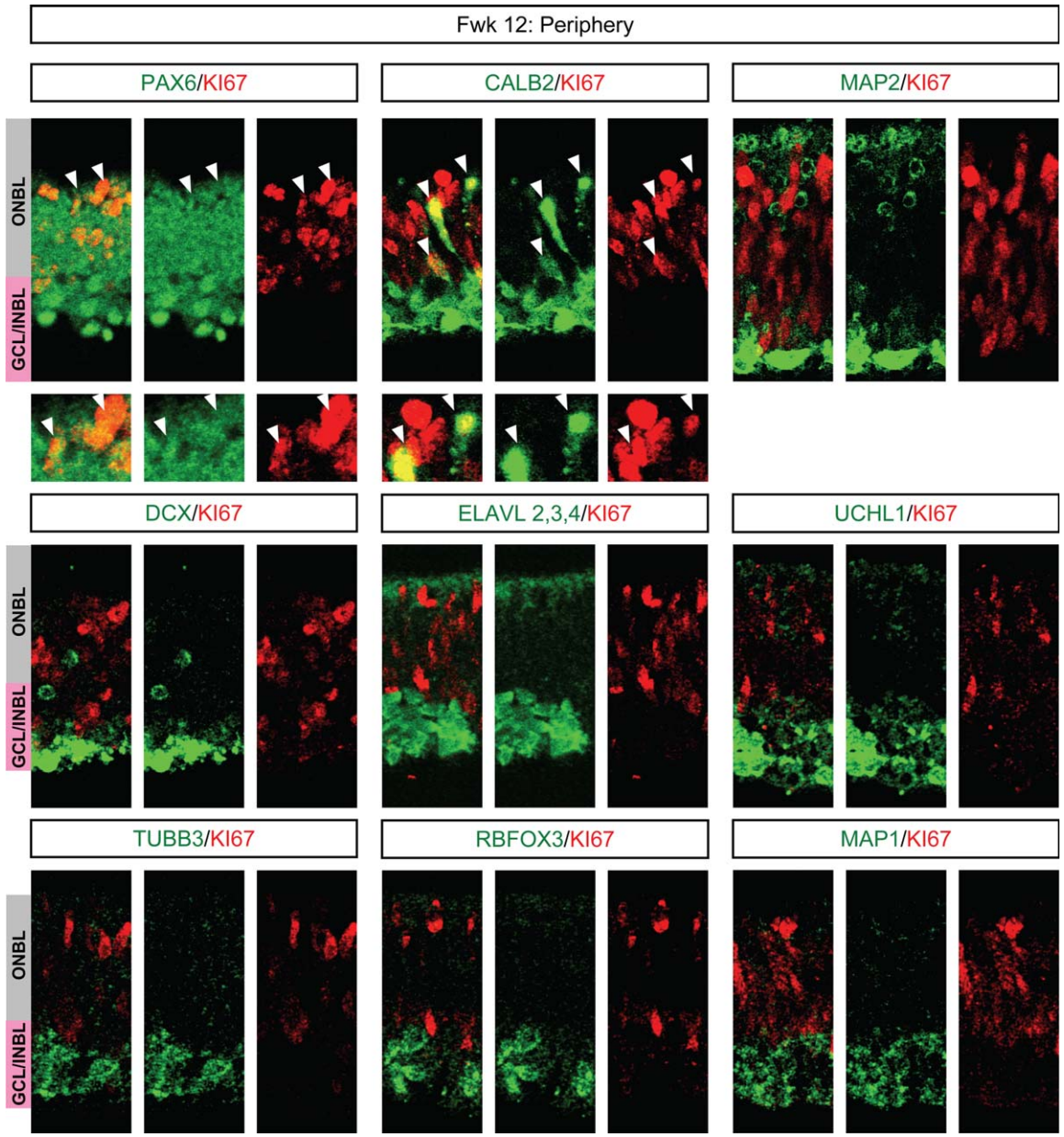

Fig. 8. CALB2, but not seven other neuronal markers, colocalizes with KI67 in the embryonic human retina. At Fwk 12, many PAX6^{+} cells (green) colocalize with KI67 (red, white arrowheads) in the ONBL, while the rest of PAX6^{+} cells are postmitotic mature neurons. A subset of Ki67^{+} cells (red) colocalizes with CALB2 (green, white arrowheads) in the ONBL, but not seven other neuronal markers (green). ONBL/INBL/GCL: outer neuroblastic layer/inner neuroblastic layer/ganglion cell layer. Scale bar = 10 μm.

retina, and TUBB3, MTAP1B, UCHL1, and RBFOX3 show delayed induction in the human tissue. Apart from their classic roles as microtubule associated proteins (TUBB3, DCX, MAP2) or calcium binding (CALB2), these proteins are also expressed in a variety of tumors, and recent studies indicate additional roles in the cell cycle and survival (Dinsmore and Solomon, 1991; Santra et al., 2006; Levallet et al., 2012; Blum and Schwaller, 2013). Similarly, the mRNA-binding ELAVL4 protein inhibits translation of the important CDK inhibitor p27 (Kullmann et al., 2002). Whether and how the cell cycle and survival functions of these proteins are used during retinal development and why their appearance would differ in mouse versus human retina is unknown. The answers to these questions will illuminate our understanding of retinal neurogenesis and may provide insight into the pathology of retinal disease and cancer.

Evidence for Biased Ganglion Cell Progenitors in Early Murine and Human Retina

Pou4f2 expression is regarded as the point at which a cell becomes committed to the ganglion cell lineage because: (a) Pou4f2 is required for ganglion cell specification, (b) Overexpression drives ganglion cell genesis, and (c) Pou4f2 is expressed only in ganglion cells (Xiang et al., 1993, 1995; Xiang, 1998; Liu et al., 2000; Qiu et al., 2008; Badea et al., 2009; Feng et al., 2011). As noted above, we find that at E12.5 in murine retina

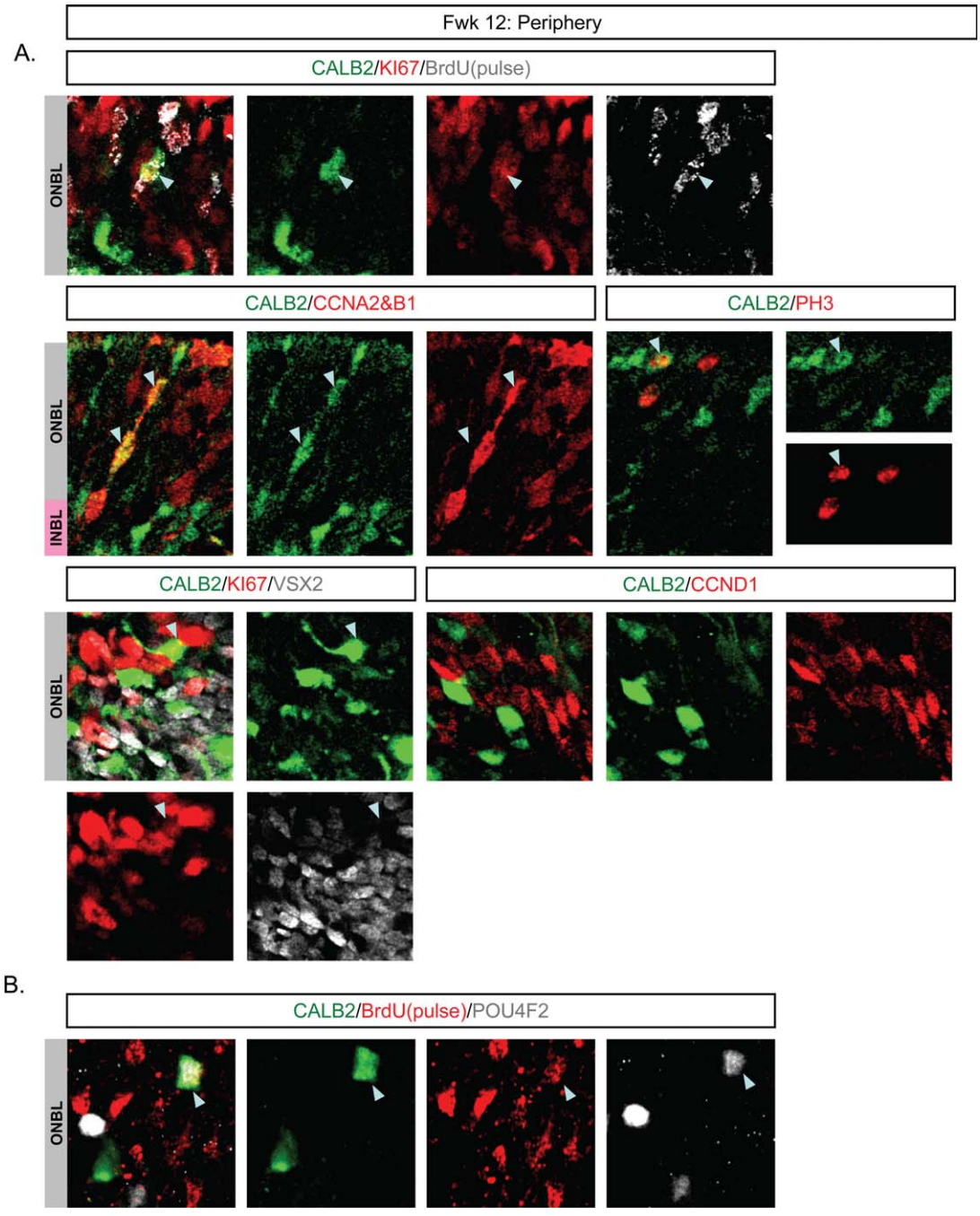

Fig. 9. CALB2 colocalizes with multiple cell cycle markers in Fwk 12 human embryonic retina. **A:** CALB2 (green) colocalizes with CCNA2, CCNB1, PH3 (all red), and a short pulse of BrdU (white), but not CCND1 (red) nor VSX2 (white). **B:** Cells colabeled for CALB2 (green) and BrdU (red) colocalize with the ganglion cell marker POU4F2 (white). INBL/ONBL/GCL: inner neuroblastic layer/outer neuroblastic layer/ganglion cell layer. Scale bar = 10 μm.

1.5% of Pou4f2^{+} or Isl1^{+} cells are labeled with a 30-min pulse of BrdU. Such a small fraction, only seen at earlier times in retinal development, would be easy to miss, and likely explains why others concluded that Pou4f2 is restricted to postmitotic cells (Xiang, 1998; Pan et al., 2005). Although small, this fraction is important because it matches the proportion of ganglion cells born in half an hour at E12.5. These findings are consistent with recent work from the Glaser lab, who also detected Pou4f2 and Isl1 in a small subset of early (<E14) but not late (>E14) S and G2/M progenitors (Brzezinski et al., 2012; Prasov and Glaser, 2012). Moreover, in retroviral lineage tracing studies the latter authors observed two-cell clones in which both neurons were ganglion cells, providing functional support for commitment before cell cycle exit. Indeed, when Brzezinski et al. delivered retroviruses at E12.5, the time point we based our calculations on, they observed that both cells in all two-cell clones obtained were ganglion cells. This finding is consistent with the notion that all E12.5 Pou4f2^{+} progenitors divide symmetrically to produce two

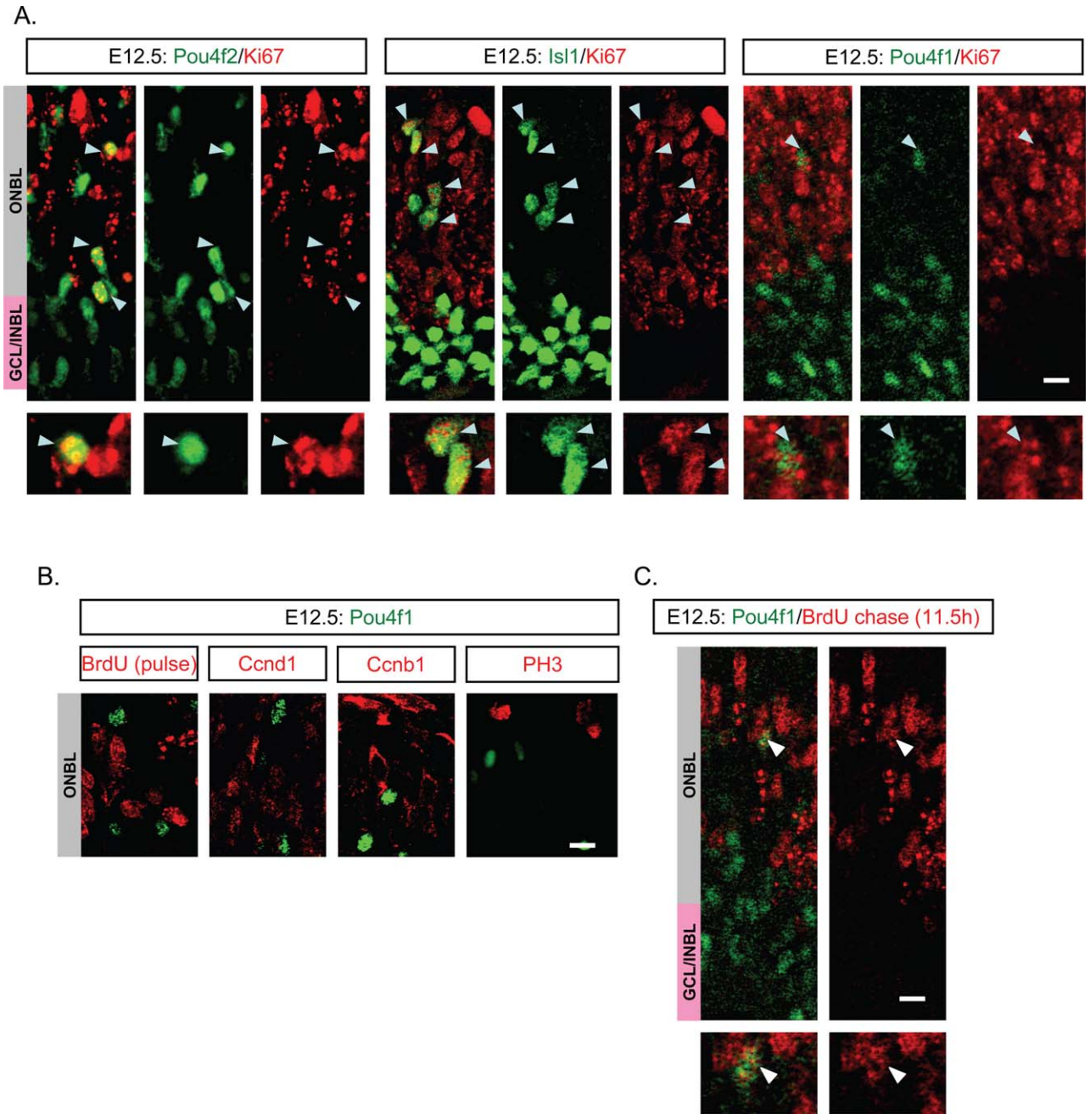

Fig. 10. Kinetics of Pou4f1, Isl1, and Pou4f2 induction in the mouse retina. **A:** Many Pou4f2$^+$ (green) and Isl1$^+$ (green) but only rare Pou4f1$^+$ (green) cells colabel with Ki67 (red) in the ONBL. **B:** Pou4f1 (green) does not colocalize with any other cell cycle markers (BrdU, Ccnd1, Ccnb1, PH3; red). **C:** BrdU chase (red) indicates that Pou4f1 (green) appears in neurons ~10 hr after G2/M. INBL/ONBL/GCL: inner neuroblastic layer/outer neuroblastic layer/ganglion cell layer. Scale bars = 10 μm.

postmitotic ganglion cells. As mentioned above, we observe that at later developmental times Pou4f2 induction shifts beyond final M-phase, and consistent with this observation Brzezinski et al. observe that after retroviral infection at E13.5 some two-cell clones contain two ganglion cells, but other contain only one ganglion cell and a different neuron. These data are all consistent with a model in which Pou4f2 induction in progenitors at E12.5 results in symmetric production of two ganglion cells, while slightly later induction at E13.5 may result in asymmetric clones. It is also feasible that asymmetric clones could result from Pou4f2$^+$ progenitors that partition the transcription factor into one of the daughters at M-phase. Indeed, in the zebrafish, progenitors expressing Ath5, the homologue of Math5/Atoh7, generate two-cell clones that partition Ath5 into one of the daughters, which always becomes a ganglion cell (Poggi et al., 2005).

Adding to this evidence for biased progenitors we report that, as in the mouse retina, a small fraction of human POU4F2$^+$ cells are also BrdU$^+$, CCNA/B$^+$, or PH3$^+$, and a similar fraction of cells expressing the neuronal marker CALB2 are also cycling progenitors. Development is considerably slower in the human vs.

TABLE 6. Induction of Murine Pou4f2, Isl1, or Pou4f1 Relative to the Cell Cycle[a]

	Ki67	BrdU chase (starting 30 min after BrdU injection)	Ccnb1	PH3	Vsx2
Marker/age	Marker$^+$; Ki67$^+$ /Marker$^+$	Marker$^+$; BrdU$^+$ /Marker$^+$	Marker$^+$; Ccnb1$^+$ /Marker$^+$	Marker$^+$; PH3$^+$ /Marker$^+$	Marker$^+$; Vsx2$^+$ /Marker$^+$
Pou4f2 (Brn3b)					
E12.5	217/477; 46.8 ± 7.2%	(0m) 19/1230; 1.5 ± 0.0% (30m) 17/800; 2.1 ± 0.2% (90m) 28/930; 3.0 ± 0.2%	3/1500; 0.2 ± 0.0%	3/1500; 0.2 ± 0.0%	0/900; 0 ± 0%
E14.5	191/670; 28.8 ± 3.7%	(90m) 5/1800; 0.2 ± 0.0% (3.5h) 25/1800; 1.3 ± 0.2% (5.5h) 64/1800; 3.5 ± 0.2% (7.5h) 90/1800; 5.0 ± 0.3% (9.5h) 117/1800; 6.5 ± 0.3%	0/900; 0 ± 0%	0/900; 0 ± 0%	0/900; 0 ± 0%
E16.5	185/670; 27.8 ± 4.5%	(7.5h) 0/1000; 0 ± 0% (9.5h) 9/770; 1.1 ± 0.3% (11.5h) 15/770; 1.9 ± 0.1%	0/900; 0 ± 0%	0/900; 0 ± 0%	0/900; 0 ± 0%
Isl1 (Islet1)					
E12.5	225/510; 45.6 ±8.1%	(0m) 20/1220; 1.6 ± 0% (30m) 17/760; 2.2 ± 0.2% (90m) 31/1020; 3.0 ± 0.2%	3/1200; 0.2± 0.1%	3/1200; 0.2± 0.1%	0/900; 0 ± 0%
E14.5	115/542; 25.8 ± 2.6%	(90m) 0/1000; 0 ± 0% (3.5h) 2/300; 0.6 ± 0.5% (7.5h) 29/300; 9.6 ± 1.5%	0/900; 0 ± 0%	0/900; 0 ± 0%	0/900; 0 ± 0%
E16.5	67/570; 11.7 ± 0.7%	(7.5h) 0/1000; 0 ± 0% (9.5h) 8/750; 1.1 ± 0.2% (11.5h) 10/770; 1.2 ± 0.5%	0/900; 0 ± 0%	0/900; 0 ± 0%	0/900; 0 ± 0%
Pou4f1 (Brn3a)					
E12.5	49/600; 8.1 ± 1.0%	(9.5h) 0/900; 0 ± 0% (11.5h) 31/1200; 2.5 ± 0.3% (23.5h) 28/580; 4.8 ± 0.2% (47.5h) 149/1130; 13.2 ± 0.9%	0/900; 0 ± 0%	0/900; 0 ± 0%	0/900; 0 ± 0%
E14.5	0/900; 0 ± 0%	(9.5h) 0/900; 0 ± 0% (11.5h) 10/600; 1.6 ± 0.2% (23.5h) 20/600; 3.3 ± 0.7% (47.5h) 41/600; 6.8 ± 0.2%	0/900; 0 ± 0%	0/900; 0 ± 0%	0/900; 0 ± 0%
E16.5	0/900; 0 ± 0%	(11.5h) 0/600; 0.0 ± 0.0% (23.5h) 19/600; 3.1 ± 1.0% (47.5h) 36/600; 6.0 ± 0.8%	0/900; 0 ± 0%	0/900; 0 ± 0%	0/900; 0 ± 0%

[a]The percentage of cells positive for three transcription factors and five cell cycle markers are shown. Note that BrdU chase time is measured starting 30 min after injection when signal is easily detectable (Pacal and Bremner, 2012), thus, when retinas were harvested 30 or 80 min after the BrdU injection, the chase is 0 or 50 min, respectively. The markers and developmental stages examined are indicated in the first column; thus, for Pax6 at E12.5, in the column labeled Ki67, of 477 Pax6$^+$ cells, 217 were also Ki67$^+$. The pale orange highlighting represents colocalization of neuronal and proliferation markers. Percentages represent the average of counts from at least three different retinas +/− SD.

murine retina, thus fewer ganglion cells would be born in any half-hour period, and indeed the fraction of POU4F2$^+$ progenitors was ~five-fold lower in human compared with mouse retina (Tables 5, 6). These cycling progenitors were CCND1 and VSX2 negative in both murine and human tissue. These data indicate that POU4F2 is induced in late stage S-phase progenitors, and thus premitotic commitment, of at least some human ganglion cells, is likely a conserved feature of ganglion cell development in these two species. Moreover, this in fact may be a common feature of vertebrate retinal development, because as mentioned above, some zebrafish progenitors are also biased to produce ganglion cells (Poggi et al., 2005).

There is growing evidence that, in addition to the ganglion cell fate, progenitors commit to other restricted cell types before cell cycle exit. For example, rat amacrine cells appear to be specified already at G2/M (Belliveau and Cepko, 1999). Furthermore, recent data show that there are distinct groups of rat progenitors that produce unique repeated patterns of daughter cell progeny (Cohen et al., 2010). Indeed, the latter work also showed that the behaviour of progenitors in culture can predict self-renewing or terminal division with 99% accuracy, or whether progenitors will produce two photoreceptors or another combination of offspring with 87% accuracy. In line with these data, recent lineage studies identified progenitors biased to producing restricted cell-types.

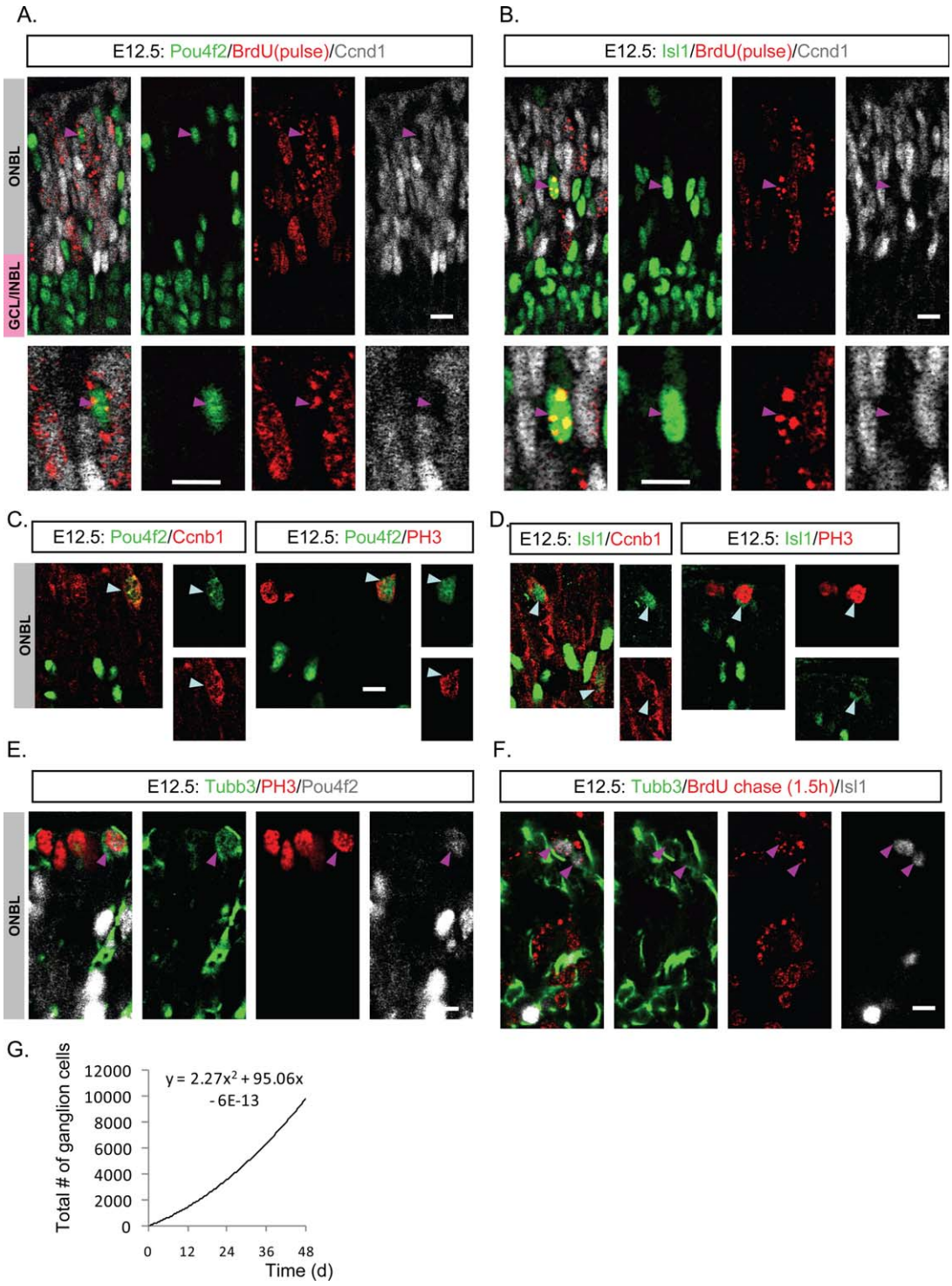

Fig. 11. Pou4f2 and Isl1 colocalize with multiple cell cycle markers in E12.5 mouse retina. **A,B:** Both Isl1 and Pou4f2 (green) are expressed in a subset of cells labelled by a short pulse of BrdU (red), indicating that they are expressed in a subset of S-phase progenitors (purple arrowheads). However, these Isl1^{+}/BrdU^{+} and Pou4f2^{+}/BrdU^{+} RPCs did not stain positive for Ccnd1 (white). Lower panels show a magnified view. **C,D:** Both Isl1 and Pou4f2 (green) were detected in some Ccnb1^{+} G2/M and PH3^{+} M cells (red, white arrowheads); larger panels show merged images, smaller panels show single colour images of the key cell. **E,F:** Pou4f2 or Isl1 (white) colocalize (purple arrows) with PH3 or a 1.5 hr BrdU chase (both red) and Tubb3 (green). **G:** The polynomial trend-line approximating the total number of ganglion cells born within the first 48 hr of mouse retinal development, modified from (Farah and Easter, 2005). INBL/ONBL/GCL: inner neuroblastic layer/outer neuroblastic layer/ganglion cell layer. Scale bars = 10 μm.

The basic helix-loop-helix (bHLH) transcription factor Ascl1 (Mash1) marks murine progenitors with a limited division capacity that give rise to all cell types except ganglion cells (Brzezinski et al., 2011). Another bHLH protein, Olig2, labels progenitors committed to terminal division; in the embryonic retina the resultant two-cell clones are primarily horizontal and cone

cells, while in the postnatal retina, they are mainly rod and amacrine cells (Hafler et al., 2012). In view of all these results, bias toward specific retinal subtypes may be a general feature of progenitors about to exit the cell cycle.

Experimental Procedures

Mice

Timed pregnant C57BL/6 (Jackson Labs) mice were used for all experiments. Noon of the day the vaginal plug was observed was considered E0.5. All mice were treated in accordance with institutional and national guidelines. At least three different mice from at least three different litters were used to generate all data. The human samples were collected and used according to a protocol approved by the research Ethics Board, Mount Sinai, Hospital, Toronto.

BrdU Labeling and Immunostaining

BrdU labeling, detection, and immunostaining was carried out as described previously (Pacal and Bremner, 2012), with the following additional details. Freshly dissected human retinal tissue was either directly fixed in 4% PFA for 12 hr, followed by dehydration in 30% sucrose for 12 hr and frozen, or incubated for 30 min–1 hr in 2 ml of culture medium (Cayouette et al., 2001) containing 1 ml of 10 mg/ml BrdU and then fixed. The human retinal sections were not subjected to antigen retrieval as we found that no antibodies required this step, with the exception of BrdU detection where sections were boiled in 10 mM sodium citrate (pH 6.0) for 15–30 min as described previously (Pacal and Bremner, 2012). Also, all antibodies were used as previously (Pacal and Bremner, 2012) except the following: Cyclin D1 (for mouse tissue: mouse, 1:100, Santa Cruz, 72-13G, SC-450; rabbit, 1:100, Santa Cruz, C-20, SC-717; for human tissue: rabbit, 1:500, Thermo Scientific, SP4, RM-9104), Pou4f1 (mouse, 1:100, Chemicon, 5A3.2, MAB1585), Pou4f2 (goat, 1:100, Santa Cruz, C-13, SC-6026), Isl1 (rabbit: 1:1000, T. Edlund, Umea U, Sweden; mouse: 1:100, Developmental Studies Hybridoma Bank, 39.4D5, Jessell, T.M. / Brenner-Morton, S.).

Imaging and Cell Counts

Images were taken with Zeiss laser confocal system and were handled with Image J (Sigma filter, z-stack manipulation) and Adobe Photoshop (image cropping, rotation, final overall intensity adjustment). All mouse retina quantifications were performed on the central (i.e., the most mature) part of the retina on a given retinal section. The quantifications of human retinal cells were performed on both peripheral and central parts as indicated, and samples from several donors (where possible) were compared and averaged. All figures represent a typical part of the retina used for scoring. Care was taken to score as many cells as possible (hundreds, sometimes thousands) to ensure statistical significance. Note that lack of staining does not automatically mean the absence of expression, but may be the result of epitope-masking or low efficiency of detection.

Acknowledgments

We thank the donors and the Morgentaler Clinic in Toronto, for providing human fetal retinal samples. This study was supported by funds to R.B. from the Canadian Institutes for Health Research, and the Foundation Fighting Blindness Canada.

References

Badea TC, Cahill H, Ecker J, Hattar S, Nathans J. 2009. Distinct roles of transcription factors brn3a and brn3b in controlling the development, morphology, and function of retinal ganglion cells. Neuron 61:852–864.

Badea TC, Nathans J. 2011. Morphologies of mouse retinal ganglion cells expressing transcription factors Brn3a, Brn3b, and Brn3c: analysis of wild type and mutant cells using genetically-directed sparse labeling. Vision Res 51:269–279.

Barishak YR. 1992. Embryology of the eye and its adnexae. Dev Ophthalmol 24:1–142.

Bassett EA, Wallace VA. 2012. Cell fate determination in the vertebrate retina. Trends Neurosci 35:565–573.

Belliveau MJ, Cepko CL. 1999. Extrinsic and intrinsic factors control the genesis of amacrine and cone cells in the rat retina. Development 126:555–566.

Blum W, Schwaller B. 2013. Calretinin is essential for mesothelioma cell growth/survival in vitro: a potential new target for malignant mesothelioma therapy? Int J Cancer 133:2077–2088.

Brzezinski JA IV, Kim EJ, Johnson JE, Reh TA. 2011. Ascl1 expression defines a subpopulation of lineage-restricted progenitors in the mammalian retina. Development 138:3519–2531.

Brzezinski JA IV, Prasov L, Glaser T. 2012. Math5 defines the ganglion cell competence state in a subpopulation of retinal progenitor cells exiting the cell cycle. Dev Biol 365:395–413.

Burmeister M, Novak J, Liang MY, Basu S, Ploder L, Hawes NL, Vidgen D, Hoover F, Goldman D, Kalnins VI ., et al. 1996. Ocular retardation mouse caused by Chx10 homeobox null allele: impaired retinal progenitor proliferation and bipolar cell differentiation. Nat Genet 12:376–484.

Cayouette M, Barres BA, Raff M. 2003. Importance of intrinsic mechanisms in cell fate decisions in the developing rat retina. Neuron 40:897–904.

Cayouette M, Poggi L, Harris WA. 2006. Lineage in the vertebrate retina. Trends Neurosci 29:563–570.

Cayouette M, Whitmore AV, Jeffery G, Raff M. 2001. Asymmetric segregation of Numb in retinal development and the influence of the pigmented epithelium. J Neurosci 21:5643–5651.

Chen D, Livne-Bar I, Vanderluit JL, Slack RS, Agochiya M, Bremner R. 2004. Cell-specific effects of RB or RB/p107 loss on retinal development implicate an intrinsically death-resistant cell-of-origin in retinoblastoma. Cancer Cell 5:539–551.

Chen D, Opavsky R, Pacal M, Tanimoto N, Wenzel P, Seeliger MW, Leone G, Bremner R. 2007. Rb-mediated neuronal differentiation through cell-cycle-independent regulation of E2f3a. PLoS Biol 5: e179.

Cohen AR, Gomes FL, Roysam B, Cayouette M. 2010. Computational prediction of neural progenitor cell fates. Nat Methods 7: 213–218.

Dinsmore JH, Solomon F. 1991. Inhibition of MAP2 expression affects both morphological and cell division phenotypes of neuronal differentiation. Cell 64:817–826.

Elshatory Y, Deng M, Xie X, Gan L. 2007. Expression of the LIM-homeodomain protein Isl1 in the developing and mature mouse retina. J Comp Neurol 503:182–197.

Ezzeddine ZD, Yang X, DeChiara T, Yancopoulos G, Cepko CL. 1997. Postmitotic cells fated to become rod photoreceptors can be respecified by CNTF treatment of the retina. Development 124:1055–1067.

Farah MH. 2004. Cumulative labeling of embryonic mouse neural retina with bromodeoxyuridine supplied by an osmotic minipump. J Neurosci Methods 134:169–178.

Farah MH, Easter SS Jr. 2005. Cell birth and death in the mouse retinal ganglion cell layer. J Comp Neurol 489:120–134.

Feng L, Eisenstat DD, Chiba S, Ishizaki Y, Gan L, Shibasaki K. 2011. Brn-3b inhibits generation of amacrine cells by binding to and negatively regulating DLX1/2 in developing retina. Neuroscience 195:9–20.

Galli-Resta L, Resta G, Tan SS, Reese BE. 1997. Mosaics of islet-1-expressing amacrine cells assembled by short-range cellular interactions. J Neurosci 17:7831–7838.

Hafler BP, Surzenko N, Beier KT, Punzo C, Trimarchi JM, Kong JH, Cepko CL. 2012. Transcription factor Olig2 defines

subpopulations of retinal progenitor cells biased toward specific cell fates. Proc Natl Acad Sci U S A 109:7882–7887.
Kullmann M, Gopfert U, Siewe B, Hengst L. 2002. ELAV/Hu proteins inhibit p27 translation via an IRES element in the p27 5'UTR'. Genes Dev 16:3087–3099.
Lee TC, Almeida D, Claros N, Abramson DH, Cobrinik D. 2006. Cell cycle-specific and cell type-specific expression of Rb in the developing human retina. Invest Ophthalmol Vis Sci 47:5590–5598.
Levallet G, Bergot E, Antoine M, Creveuil C, Santos AO, Beau-Faller M, de Fraipont F, Brambilla E, Levallet J, Morin F., et al. 2012. High TUBB3 expression, an independent prognostic marker in patients with early non-small cell lung cancer treated by preoperative chemotherapy, is regulated by K-Ras signaling pathway. Mol Cancer Ther 11:1203–1213.
Liu W, Khare SL, Liang X, Peters MA, Liu X, Cepko CL, Xiang M. 2000. All Brn3 genes can promote retinal ganglion cell differentiation in the chick. Development 127:3237–3247.
Livesey FJ, Cepko CL. 2001. Vertebrate neural cell-fate determination: lessons from the retina. Nat Rev Neurosci 2:109–118.
MacPherson D, Sage J, Kim T, Ho D, McLaughlin ME, Jacks T. 2004. Cell type-specific effects of Rb deletion in the murine retina. Genes Dev 18:1681–1694.
Mizeracka K, DeMaso CR, Cepko CL. 2013. Notch1 is required in newly postmitotic cells to inhibit the rod photoreceptor fate. Development 140:3188–3197.
Mu X, Fu X, Beremand PD, Thomas TL, Klein WH. 2008. Gene regulation logic in retinal ganglion cell development: Isl1 defines a critical branch distinct from but overlapping with Pou4f2. Proc Natl Acad Sci U S A 105:6942–6947.
Nag TC, Wadhwa S. 1999. Developmental expression of calretinin immunoreactivity in the human retina and a comparison with two other EF-hand calcium binding proteins. Neuroscience 91:41–50.
Pacal M, Bremner R. 2012. Mapping differentiation kinetics in the mouse retina reveals an extensive period of cell cycle protein expression in post-mitotic newborn neurons. Dev Dyn 241:1525–1544.
Pan L, Deng M, Xie X, Gan L. 2008. ISL1 and BRN3B co-regulate the differentiation of murine retinal ganglion cells. Development 135:1981–1990.
Pan L, Yang Z, Feng L, Gan L. 2005. Functional equivalence of Brn3 POU-domain transcription factors in mouse retinal neurogenesis. Development 132:703–712.
Poggi L, Vitorino M, Masai I, Harris WA. 2005. Influences on neural lineage and mode of division in the zebrafish retina in vivo. J Cell Biol 171:991–999.
Prasov L, Glaser T. 2012. Dynamic expression of ganglion cell markers in retinal progenitors during the terminal cell cycle. Mol Cell Neurosci 50:160–168.
Provis JM, van Driel D, Billson FA, Russell P. 1985. Development of the human retina: patterns of cell distribution and redistribution in the ganglion cell layer. J Comp Neurol 233:429–451.
Qiu F, Jiang H, Xiang M. 2008. A comprehensive negative regulatory program controlled by Brn3b to ensure ganglion cell specification from multipotential retinal precursors. J Neurosci 28:3392–3403.
Rowan S, Cepko CL. 2004. Genetic analysis of the homeodomain transcription factor Chx10 in the retina using a novel multifunctional BAC transgenic mouse reporter. Dev Biol 271:388–402.
Sangwan M, McCurdy SR, Livne-Bar I, Ahmad M, Wrana JL, Chen D, Bremner R. 2012. Established and new mouse models reveal E2f1 and Cdk2 dependency of retinoblastoma, and expose effective strategies to block tumor initiation. Oncogene 31:5019–5028.
Santra M, Zhang X, Santra S, Jiang F, Chopp M. 2006. Ectopic doublecortin gene expression suppresses the malignant phenotype in glioblastoma cells. Cancer Res 66:11726–11735.
Sidman RL. 1961. Histogenesis of mouse retina studied with thymidine-H3. In GK Smelster, editor. The structure of the eye. New York: Academic Press.
Workman AD, Charvet CJ, Clancy B, Darlington RB, Finlay BL. 2013. Modeling transformations of neurodevelopmental sequences across mammalian species. J Neurosci 33:7368–7683.
Xiang M. 1998. Requirement for Brn-3b in early differentiation of postmitotic retinal ganglion cell precursors. Dev Biol 197:155–169.
Xiang M, Zhou L, Macke JP, Yoshioka T, Hendry SH, Eddy RL, Shows TB, Nathans J. 1995. The Brn-3 family of POU-domain factors: primary structure, binding specificity, and expression in subsets of retinal ganglion cells and somatosensory neurons. J Neurosci 15(pt 1):4762–4785.
Xiang M, Zhou L, Peng YW, Eddy RL, Shows TB, Nathans J. 1993. Brn-3b: a POU domain gene expressed in a subset of retinal ganglion cells. Neuron 11:689–701.
Young RW. 1985. Cell differentiation in the retina of the mouse. Anat Rec 212:199–205.